DOI: 10.1002/chem.200700181

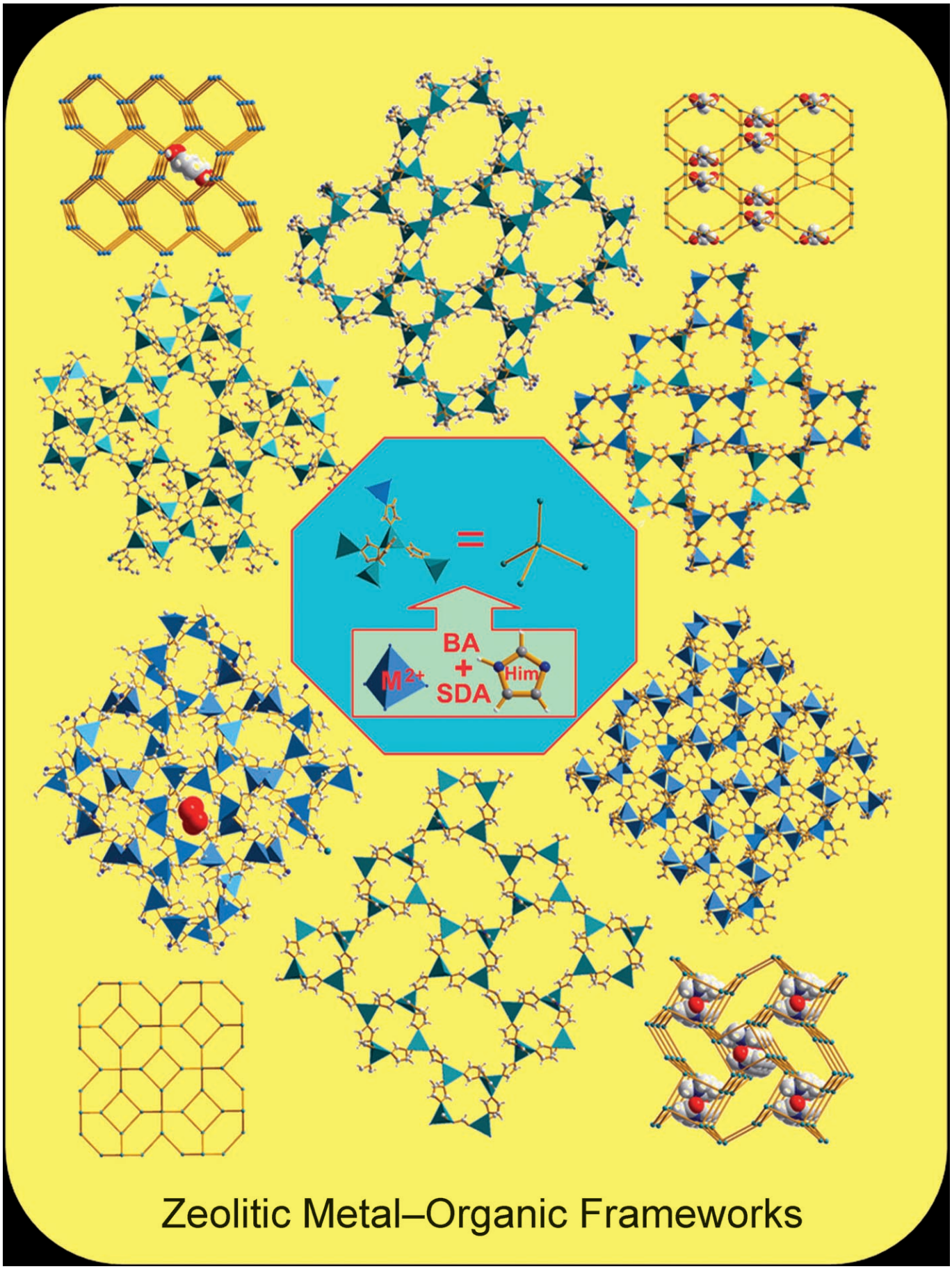

# Design and Generation of Extended Zeolitic Metal–Organic Frameworks (ZMOFs): Synthesis and Crystal Structures of Zinc(II) Imidazolate Polymers with Zeolitic Topologies

**Yun-Qi Tian,*[a] Yu-Ming Zhao,[a] Zhen-Xia Chen,[b] Guang-Ning Zhang,[a] Lin-Hong Weng,[b] and Dong-Yuan Zhao[b]**

**Abstract:** Attempts to create metal–organic frameworks (MOFs) with zeolitic topologies, metal (zinc(II) and cobalt(II)) imidazolates have repeatedly been used as the metal–organic motifs of inorganic silicate analogues. By modulating the synthetic strategy based on the solvothermal and liquid diffusion method, seven further MOFs (including at least three zeolitic MOFs) of zinc(II) imidazolates, $[Zn(im)_2 \cdot x\,G]$ (G = guest molecule, $x = 0.2$–1) **1a**–**7a**, have been successfully synthesized. Of these, **1a**–**3a** are isostructural with the previously reported cobalt analogues **1b**–**3b**, respectively, while **4a**–**7a** are new members of the metal imidazolate MOF family. Complex **4a** exhibits a structure related to silicate $CaAl_2Si_2O_8$ of $CrB_4$ topology, but with a higher network symmetry; complex **5a** has a structure with zeolitic DFT topology that was discovered in zeolite-related materials of DAF-2, UCSB-3, and UCSB-3GaGe; complex **6a** demonstrates an unprecedented zeolite-like topology with one dimensional channels with 10-rings; and **7a** displays a structure of natural zeolite GIS (gismondine) topology. All of these polymorphous MOFs were created only by using certain solvents as structure-directing agents (SDAs). Further extensive metal–organic frameworks with zeolitic topologies can be envisaged if other solvents were to be used.

**Keywords:** coordination polymers · imidazolates · solid-state structure · zeolite analogues · zinc

## Introduction

Metal–organic frameworks (MOFs) with mineral topologies have been widely explored since 1990.[1] However, as the natural choice for porous materials, the topologies of zeolites are still very difficult to realize in MOFs: this remains a great challenge[2] although zeolite MTN (Mobile Thirty Nine),[3] SOD (sodalite)[4] and ABW[5] topologies have been successfully recreated in MOFs that only consist of a tiny part of all the zeolitic (zeolite and zeolite-like) structures explored.[6] Therefore, in order to fabricate MOFs with more extensive zeolitic topologies, understanding the key issues that influence the formation of extensive zeolitic structures is crucial.

Since the discovery of high-silica molecular sieves, such as ZSM-5 and silicalites, a high proportion of alumina had not been thought to be a key component in the formation of the diverse porous architectures of zeolites.[7] In fact, that should depend on the inherent structural features of the zeolitic primary building unit (PBU), namely the corner-sharing tetrahedral $TO_4$ (T = Si or Al, O-T-O = 109.5°, T-O-T = 145° in which the T–O bonds could freely rotate). It is this type of PBU that endows the zeolites with the flexibility of T-T-T angles and also make possible the various secondary building units (SBUs) and coplanar T-atom rings with 4- to 10-members.[8] Thus, the creation of MOFs with augmented zeolitic structures is not due to the augmentation of a specialized zeolitic structure, but rather to the augmentation of the PBU of the zeolites. Cobalt(II) and zinc(II) imidazolate polymers were chosen as the ideal metal–organic analogues of inorganic silicates as their PBU, $[M(im)_4]$

[a] Prof. Dr. Y.-Q. Tian, Y.-M. Zhao, G.-N. Zhang
Institute of Chemistry for Functionalized Materials
College of Chemistry and Engineering
Liaoning Normal University
Huang-He Road 850, Dalian 116029 (China)
Fax: (+86) 411-82156858
E-mail: yqtian@lnnu.edu.cn

[b] Z.-X. Chen, Prof. Dr. L.-H. Weng, Prof. Dr. D.-Y. Zhao
Department of Chemistry, Fudan University
Handan Road 220, Shanghai 200433 (China)

Supporting information for this article is available on the WWW under http://www.chemistry.org or from the author.

  

($M=Co^{2+}$, $Zn^{2+}$), is structurally similar to the $TO_4$ of zeolites and they can be regarded as the metal–organic motifs of the augmented $TO_4$ (Scheme 1). Even though the extend-

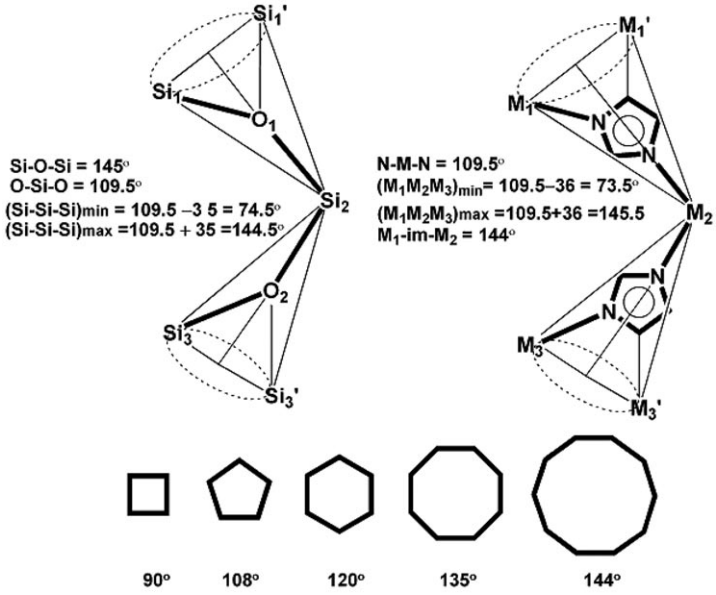


Scheme 1. Schematic display of the flexibility of the T-T-T angles in silicates and zinc (or cobalt) imidazolate polymers (only three neighbouring T-atoms are selected for clarity).

ed frameworks of cobalt(II) imidazolates[9] (as well as some of copper(II) imidazolates or metal–diazolates[10]) are structurally reminiscent of the zeolitic features, we are aiming at creating extended ZMOFs (ZMOF = zeolitic MOF). We have always firmly believed that most of the zeolitic topologies can be fabricated with metal imidazolates if effective synthetic strategies are employed.[9b,c] For example, Chen and co-workers[11] successfully acquired three MOFs of zinc(II) 2-alkylimidazolates with zeolite SOD, ANA, and RHO topologies by the introduction of different small substituents that play the roles of the templates and structure-directing agents (SDAs) to the imidazolate ligands. At almost the same time, Eddaoudi and co-workers[12] also realized the SOD- and RHO-topological MOFs with another metal imidazolate derivate, the indium 4,5-imidazoledicarboxylate. Based on our earlier research, we decided to use the cobalt and zinc imidazolates as an analogy of inorganic silica. By employing a proper buffering agent (BA) that enables the crystallization of metal imidazolates at room-temperature, a strategy for the nonsolvothermal synthesis has been established. With recourse to proper solvents as the templates or the SDAs, further extended MOFs including the ZMOFs of metal(II) imidazolates have been achieved. Thus, extended ZMOFs have been intentionally realized by the more or less deliberate crystal engineering. The isomeric and isocrystalline MOFs of the zinc(II) and cobalt(II) imidazolates reported in this paper have the general formula $[M(im)_2 \cdot x\,G]$; see Table 1 for specific details.[9]

Table 1. Nomenclature used for the $[M(im)_2 \cdot x\,G]$ complexes (M = metal, G = guest molecule) reported in this paper.

| | Metal | Guest[a] | $x$ |
|---|---|---|---|
| **1a** | Zn | DEF/MB | 0.2–0.4 |
| **2a** | Zn | DMA/NMP | 0.5 |
| **3a** | Zn | DMF | 0.5 |
| **4a** | Zn | DMF | 1.5 |
| **5a** | Zn | DMF/DMA/NMP | 1 |
| **6a** | Zn | DEF | 0.2–0.4 |
| **7a** | Zn | DEF | ? |
| **1b** | Co | DEF/MB | 0.2–0.4 |
| **2b** | Co | DMA | 0.5 |
| **3b** | Co | DMA | 0.5 |

[a] DEF = diethylformamide, MB = 3-methyl-1-butanol, DMA = dimethylacetamide, DMF = dimethylformamide, NMP = *N*-methylpyrrolidone.

## Results and Discussion

**Crystal structures of the zinc(II) imidazolate polymers**: The MOFs of zinc(II) imidazolates $[Zn(im)_2 \cdot x\,G]$ were determined by single-crystal X-ray diffraction (Table 2). Of them, compounds **4a–7a** are new members of the metal imidazolate family, while **1a–3a** are isostructural with their cobalt analogues **1b–3b** (M = Co), respectively, which we have previously reported.[9] The structures of the above-mentioned zinc(II) imidazolates exhibit the polymorphous MOFs of four-connected networks: each zinc in the MOFs is coordinated with four imidazolate nitrogen atoms and each imidazolate ligand links two zinc ions (Zn-im-Zn) into three-dimensional frameworks (Table 3) that show the structural features of zeolitic (4,2)-net[14,15] just like the MOFs of cobalt(II) imidazolates solvothermally synthesized.[9a,c]

Complex **4a** (Figure 1) crystallizes in an orthorhombic structure and its framework relates to that of $CaAl_2Si_2O_8$ with $CrB_4$ topology, which appears also in **2a**. However, with the space group *Pbca*, it has a symmetry higher than $P2_1/n$ of **2a**. The framework density of **4a** is lower than that of **2a** and therefore accommodates more guest molecules than **2a**: in addition to the DMF molecules encapsulated in each of the $4^26^4$-cage units, DMF molecules are also accommodated in the 8-ring channels, which are $12.7 \times 12.7$ Å in diameter (if the imidazolate ligands and Van der Waal radii are taken into account, the effective opening is $7.3 \times 7.3$ Å). Complex **4a** reveals a framework density of $0.921\ g\,cm^{-3}$ and the accessible space to guests of 47.4%. The relationship between **4a** and **2a** is very similar to that between β-quartz and α-quartz, which have the same framework topology but different framework symmetries and densities.

Complex **5a** (Figure 2) crystallizes in a tetragonal form with a space group $P4_2/mnm$ and its framework demonstrates the zeolitic DFT topology, which has been found so far only in the zeolite-related materials such as DAF-2 (a cobalt phosphate),[16] UCSB-3 (a zinc arsenate)[17] and UCSB-3GaGe (a gallium germanate).[18] The SBU of **5a** is a 4-ring of $Zn_4$ linked by imidazolates, from which the subunits of Narsarsukite chains (or bifurcated hexagon plus square (bhs) chains) are constructed. These chains run in

  

Table 2. Crystal data of the metal imidazolates.

| | **1a** | **2a** | **3a** | **4a** | **5a** | **6a** | **7a** |
|---|---|---|---|---|---|---|---|
| | $[Zn_5(im)_{10}\cdot DEF]$ | $[Zn_2(im)_4\cdot DMA]$ | $[Zn_2(im)_4\cdot DMF]$ | $[Zn_2(im)_4\cdot 3DMF]$ | $[Zn(im)_2\cdot H_2O]$ | $[Zn_5(im)_{10}\cdot DEF]$ | $[Zn(im)_2]$ |
| formula | $Zn_5C_{40}H_{52}N_{22}O_2$ | $Zn_2C_{16}H_{21}N_9O$ | $Zn_2C_{15}H_{19}N_9O$ | $Zn_2C_{21}H_{33}N_{11}O_3$ | $C_{11}H_{17}N_5O_2Zn$ | $Zn_5C_{40}H_{52}N_{22}O_2$ | $ZnC_6H_6N_4$ |
| *Fw* | 1199.89 | 486.16 | 472.13 | 618.32 | 316.69 | 1199.89 | 199.52 |
| space group | $P2_1/n$ | $P2_1/n$ | *Pbca* | *Pbca* | $P4_2/mnm$ | $C2/c$ | $I4_1/a$ |
| crystal system | monoclinic | monoclinic | orthorhombic | orthorhombic | tetragonal | monoclinic | tetragonal |
| *a* [Å] | 24.359(5) | 9.750(7) | 15.379(5) | 9.801(3) | 19.073(9) | 37.241(11) | 18.389(4) |
| *b* [Å] | 9.6097(19) | 15.268(10) | 15.449(5) | 24.104(8) | 19.073(9) | 19.217(6) | 18.389(4) |
| *c* [Å] | 24.804(5) | 14.971(10) | 18.407(6) | 24.356(8) | 17.058(12) | 25.547(8) | 19.129(5) |
| $\alpha$ [°] | 90.00 | 90.00 | 90.00 | 90.00 | 90.00 | 90.00 | 90.00 |
| $\beta$ [°] | 91.774(4) | 98.584(9) | 90.00 | 90.00 | 90.00 | 132.410(3) | 90.00 |
| $\gamma$ [°] | 90.00 | 90.00 | 90.00 | 90.00 | 90.00 | 90.00 | 90.00 |
| $V$ [Å$^3$] | 5803(2) | 2204(3) | 4373(2) | 5754(3) | 6205(6) | 13499(7) | 6469(2) |
| $Z$ | 4 | 4 | 8 | 8 | 16 | 8 | 16 |
| $\rho$ [g cm$^{-1}$] | 1.258 | 1.465 | 1.434 | 1.428 | 0.931 | 1.081 | 0.819 |
| $\mu$ [mm$^{-1}$] | 2.080 | 2.201 | 2.216 | 1.709 | 1.559 | 1.788 | 1.487 |
| $wR_2$ ($F^2$ all data) | 0.1804 | 0.1831 | 0.1362 | 0.1858 | 0.2245 | 0.2194 | 0.1929 |
| $R_1$ [$I>2\sigma(I)$] | 0.0550 | 0.0749 | 0.0424 | 0.0608 | 0.0687 | 0.0692 | 0.0629 |
| GOF | 1.006 | 1.052 | 1.071 | 1.045 | 1.042 | 1.015 | 0.988 |

Table 3. Synthetic and structural information of metal imidazolates.

| MOFs | **1a** | **2a** | **3a** | **4a** | **5a** | **6a** | **7a** |
|---|---|---|---|---|---|---|---|
| SDA | DEF | DMA,NMP | DMF | DMF | DMF,DMA,NMP | DEF | DEF |
| BA | propylamine | propylamine | propylamine | propylamine | propylamine | propylamine | propylamine |
| topology | zeolite-like | $CrB_4$ | $CaGa_2O_4$ | $CrB_4$ | zeolitic DFT | zeolite-like | zeotype GIS |
| FD [g cm$^{-3}$][a] | 1.105 | 1.203 | 1.212 | 0.921 | 0.841 | 0.982 | 0.819 |

[a] FD: Framework density.

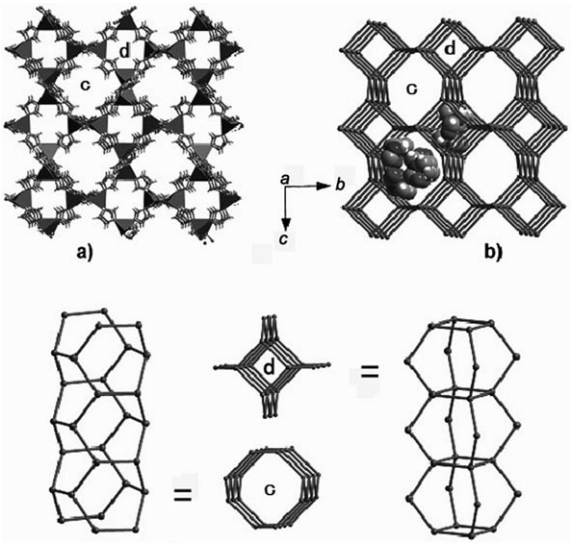


Figure 1. a) Polyhedral diagram of **4a** along [100] direction; b) Ball-and-stick diagram of **4a** along [100] direction (the space-filling diagrams represent guest DMF molecules) in which **c** is a tubular building unit with 8-ring opening and **d** is a building unit of $6^4 4^2$-cage chain of the topological framework of **4a**.

the [001] direction and connect with each other by linking their four-connection nodes into a three-dimensional network. The DFT structure is characterized by one set of

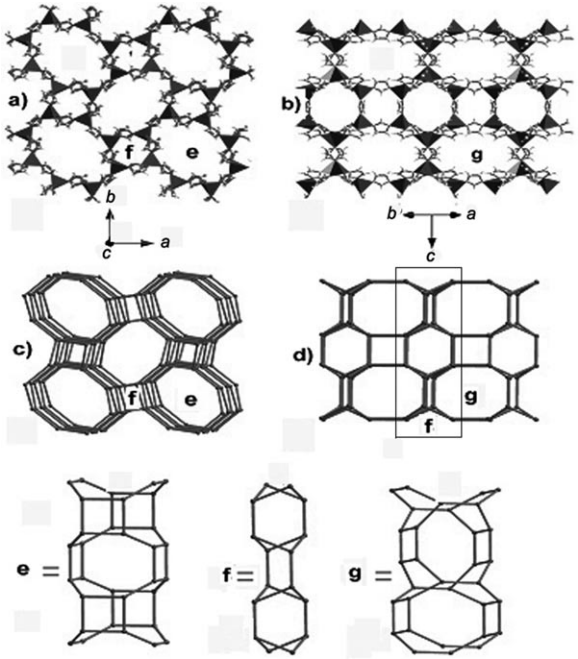


Figure 2. a) and b) Polyhedral diagram of **5a** along the [001] and [110] directions, respectively; c) and d) Ball-and-stick diagram of **5a** along the [001] and [110] directions, respectively, in which **e** indicates the channel formed by a tubular building unit with side windows, **f** is the second building unit (SBU) of bifurcated hexagon plus square (bhs) chain (Narsarsukite chain) of the DFT frameworks and **g** indicates the channel formed by another tubular building unit with side windows.

  

channels with an elliptical 8-ring opening of 16.0×12.1 Å (free opening of 11.5×5.8 Å) in [001] direction and two sets of identical channels with openings of 16.0×11.0 Å (free aperture 10.1×6.5 Å) in the [110] and [1$\bar{1}$0] directions, respectively. The channels in the [110] and [1$\bar{1}$0] directions do not intersect each other; however, they do intersect with those running in the [001] direction. The solvent molecules of DMF, DMA or NMP are too small to be captured firmly in these large intersected three-dimensional channels of **5a**; therefore, apart from a few disordered oxygen atoms from the moisture, the highly mobile guest molecules could not be detected in the crystal determination although they do exist in the MOFs according to the IR spectra, and elemental and thermogravimetric (TG) analyses. Complex **5a** reveals the framework density of 0.841 g cm$^{-3}$ and space accessible to guests about 52.0%.

Complex **6a** crystallizes in a monoclinic structure with space group *C*2/*c* (Figure 3). The SBUs of **6a** are 4- and 6-rings of zinc(II) imidazolate: from the 4-rings the subunit of a double-crankshaft chain (cc) is built up and from the 4- and 6-rings a chain that had never been observed in zeolites and zeolite-related materials is constructed. We name this chain "double-twisted-hexagon chain (thth)" (following the name of twisted square chain in zeolites[19]). The thth chains running in the [001] direction intersect with the cc chains running in the [010] direction by sharing the 4-rings on the peaks of cc chains, giving rise to an unprecedented three-dimensional zeolite-like network. Complex **6a** has one-dimensional 10-ring channels with 20.6×12.6 Å openings (effective opening of 16.4×9.8 Å) running in the [001] direction. There ought to be guest molecules accommodated in these channels according to the results of TG and elemental analyses, but they evaded X-ray determination due to their high level of disorder. Only those located in the $4^2 6^4$-cages were detected by single-crystal X-ray determination. So far, the 10-ring is the largest channel-opening found in MOFs of zinc(II) and cobalt(II) imidazolates, but certainly, this will not be the largest. Complex **6a** has a framework density of 0.982 g cm$^{-3}$ and a space accessible to guests approximately 44.5%.

Complex **7a** (Figure 4) crystallizes in a tetragonal form with a space group $I4_1/a$. The SBU of this framework is the 4-ring, from which the cc chain is constructed. These cc chains, which propagate in the [100] direction, intersect with those running in the [010] direction by using the common 4-rings on the peaks to form a three-dimensional network. The **7a** can also be described as 4- and 8-ring SBUs, from which the subunits of (4.8.8)-sheets[19] are formed. These sheets of three-connected nodes parallel to (100) {or (010)} plane are linked with each other up and

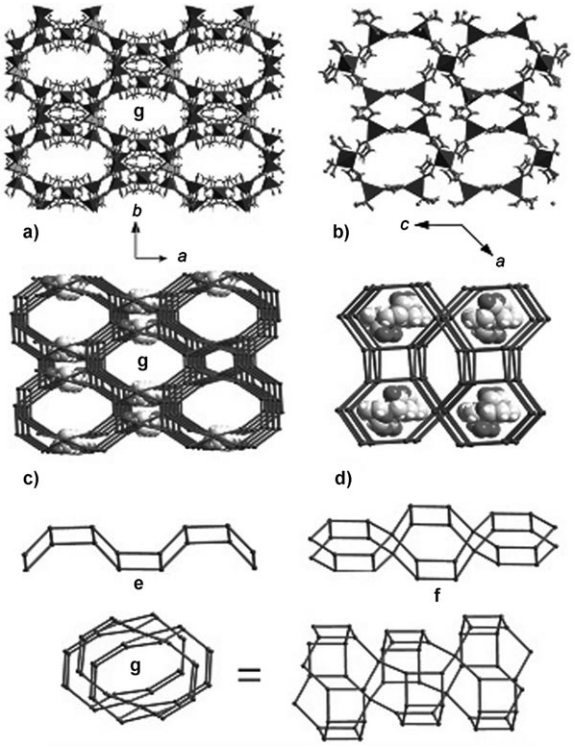


Figure 3. a) and b) Polyhedral diagram of **6a** along the [001] and [010] directions, respectively; c) and d) Ball-and-stick diagram of **6a** along the [001] and [010] directions, respectively, in which **e** is the SBU of double crankshaft chain (cc), **f** the SBU of double-twisted-hexagon chain (thth) and **g** indicates the channel formed by a tubular building unit with 10-ring opening.

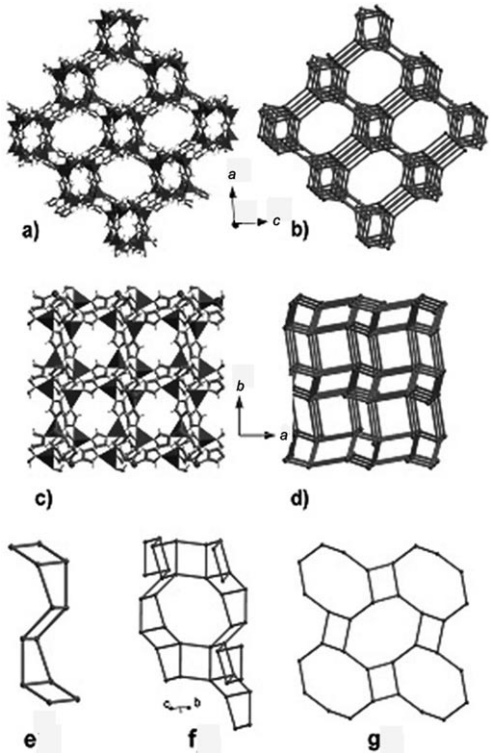


Figure 4. a) and b) Polyhedral and ball-and-stick diagram of **6a** along the [010] direction; c) and d) Polyhedral and ball-and-stick diagram of **6a** along the [001] direction, in which **e** is the SBU of double crankshaft chain (cc) of the GIS framework, **f** is a fragment of the GIS framework with 8-ring pore formed by intersected cc-chains and **g** reveals the 4.8.8 sheet of zeolite GIS topological structure.

down in the [100] {or [010]} direction, giving rise to a three-dimensional network by completing the four-connection of the nodes. This is exactly the network related to zeolite GIS (gismondine) topology.[20–22] With the topology of natural zeolite GIS, **7a** consists of identical channels of 8-ring openings in the [100] and [010] directions. These channels intersect each other form a three-dimensional channel with inner passage gates of $17.5\times12.9$ Å (effective opening of $10.4\times8.7$ Å) in which no guest molecule could be detected by the single crystal X-ray determination. However, it may be similar to the case of **5a** and **6a** with highly disordered guest molecules, which also evaded X-ray detection. This ZMOF has a framework density of 0.819 $g cm^{-3}$ and a space accessible to guests about 53.4%.

**The nonsolvothermal synthesis of metal imidazolates**: The piperazine-buffered solvothermal method[9,13] has proved to be a successful synthetic strategy for generating extended silica-like frameworks of cobalt(II) (and zinc(II)) imidazolates. However, according to the solvothermal mechanism we previously demonstrated,[13] the solvothermal temperature should not be lower than 100°C, otherwise, the piperazine molecules cannot release the metals for generating the metal imidazolates. Moreover, at such a temperature, molecules with a low boiling point involved in the reactions (such as water) may generate high pressure in autoclaves that does not benefit generation of the MOFs with low framework density, the potential ZMOFs. It was noted that **1b**, the only ZMOF of metal imidazolates prepared solvothermally,[9a] has a framework density of 1.105 $g cm^{-3}$. Thereby, to realize the intended metal imidazolates with the most expected ZMOFs of low framework-density, a strategy has to be developed of seeking new organic bases which could buffer the metal imidazolate formation at room or even lower temperature so that the nonsolvothermal synthesis (liquid-diffusion and liquid-mixing at room-temperature) could be then available. Fortunately, primary organic amines or aqueous ammonia are the candidates as BAs for the nonsolvothermal synthesis, of them the propylamine is the best one (using aqueous ammonia often makes organic solvents lose their structure-directing effect due to the volume of water introduced into the reactant mixtures that may further lead to generation of even more dense MOFs, such as the one with a network topology of banalsite[9b]). If that happens, a nonsolvothermal mechanism such as that in Scheme 2 can be proposed. Thus, with recourse to the correct solvents as templates or SDAs, various MOFs and ZMOFs of zinc(II) imidazolate polymers can be produced, for which the single crystals are formed by liquid diffusion and the bulk microcrystals by liquid mixing. Here, it is worth noting that we have failed to produce the MOFs of cobalt(II) imidazolate by using the new synthetic strategy, since an amorphous solid is always produced.

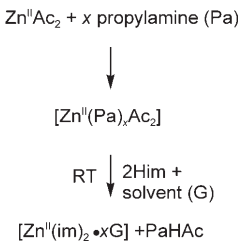


Scheme 2. The nonsolvothermal route of the zinc(II) imidazolate synthesis.

**The template or structure-directing effect of some organic solvents**: In the hydrothermal synthesis of zeolites, the synthetic variables are templates (organic amines), temperature, Si/Al ratio and their concentrations in the reactant mixture. Of these variables, the organic amines play very important roles in 1) structure-direction or templation, 2) gel modification, and 3) gel-PH alteration or buffering. Correspondingly in the solvothermal or nonsolvothermal synthesis of metal imidazolates, the organic amines play only the roles of 1) the bases for deprotonation of imidazole and 2) the buffering ligands for ready release of metal ions. So far, no amine has been discovered that has a template effect in the synthesis of metal imidazolates, but those organic solvents with strong solvating effect, such as dimethylformamide (DMF), dimethylacetamide (DMA), diethylformamide (DEF) and *N*-methylpyrrolidone (NMP) have played the template or structure-directing agent (SDA) roles. They have led to generation of extended MOFs and ZMOFs of zinc(II) imidazolates (Table 3).

By using DMF as a solvent, crystals of three MOFs of **3a**, **4a**, and **5a** were produced by the liquid-diffusion method. Of them only pure **3a** could be acquired, while **4a** and **5a** were often generated near the start of the liquid-diffusion process and then they transformed into **3a**. Therefore, the single crystals of **4a** and **5a** suitable for X-ray diffractions could only be isolated as we decreased the reaction temperature below 15°C. Otherwise, these crystals would transform into the MOF of **3a** before they grew to a size suitable for the single-crystal determination. Thereupon, we name **3a** the thermodynamically controlled MOF, while the others are the dynamically controlled ones of the DMF-directed products.

By using DMA as solvent in the liquid-diffusion process, single crystals of **2a** and **5a** were produced. Similar to the case above, **5a** is a dynamically controlled MOF, while **2a** a thermodynamically controlled MOF of the DMA-directed structures.

When we used DEF as solvent in the liquid-diffusion process, single crystals of at least five structures could be obtained. Of these only the structures of **1a**, **6a** and **7a** were crystallographically solved and refined, while the other two still cannot be fully solved due to the poor quality X-ray diffraction data. In the MOFs of DEF-directed products, **1a** was the thermodynamically controlled MOF. Complex **6a** should be a thermodynamically controlled quasi-stable MOF, because, similar to **2a** and **3a**, it can be always obtained as single phase by the liquid mixing. However, as the concentration of the reactants was increased and the reaction time was prolonged, **1a** was the final product. These results tally with the result of the corresponding solvothemal synthesis when DEF is used as the solvent.

It is interesting that the pure phase of **5a** can be obtained by both liquid diffusion and liquid mixing when NMP is used as a solvent. It seems that NMP is the best-matching

  

template for generation of **5a**; however, the NMP molecules are presumably highly disordered and thus evade the X-ray detection, since the results of IR spectra, and elemental and TG analyses evidenced that they do exist in the MOFs. Evidently, there are no matching cages or holes for the NMP molecules in **5a**; therefore, it is reasonable to regard NMP as an SDA rather than a template. Thus, **5a** should be a thermodynamically controlled quasi-stable MOF of the NMP-directed structures. This was then confirmed by the solvothermal synthesis using NMP as a solvent that produced **2a**, which should be the thermodynamically controlled MOF of NMP-directed structures.

**The effect of M–N bond rotation flexibility**: To establish the flexibility of M–N bond rotation as another key for generating extended MOFs of metal imidazolates, we introduced the small methyl group into the imidazolate ring to see whether the extended MOFs could also be generated by employing different solvents as SDAs. The experiments revealed that only the MOF reported by Chen et al. with sodalite (SOD) structure[11] can be produced no matter which SDA in combination with propylamine (or aqueous ammonia) are employed. Evidently, the substituent methyl group plays the template and SDA role in the synthesis. However, it restricts the flexibility of the Zn–N bond rotation and thus leads to the metal 2-methylimidazolate suffering from a lack of framework diversity. Nevertheless, the methyl groups as the inseparable supporting templates can enhance sodalite MOF with high thermal stability: that is why the MOF free from guests can be produced even under the solvothermal condition.

**Thermal stabilities of the MOFs of zinc imidazolate**: To study the thermal stability of the zinc(II) imidazolates, thermogravimetric analyses (TGA) were carried out for the MOFs of zinc(II) imidazolates (see Supporting Information) except for **4a** and **7a**. Even though the TGA results show that none of the MOFs experiences weight-loss from about 250 up to 450 °C after total liberation from guest molecules, the results of their XRD measurements indicate that only **1a** retains its structure after losing the guest molecules, while the others lose their crystalline integrity and become dense structural or amorphous solids, especially if a trace amount of propylamine is present. To try and realize the evacuated zinc(II) imidazolates retaining their original crystalline integrity, we attempted to evacuate the as-synthesized samples below 100 °C in vacuum; however, the crystalline integrity was again not retained after losing the guest molecules.

## Conclusions

To create MOFs with zeolitic topologies, we decided to use metal imidazolates as the metal–organic analogues of inorganic silica. For generation of these ZMOFs, the strategy of nonsolvothermal synthesis has been developed by employing a room-temperature buffering method. By recourse to a number of solvents, such as DMF, DMA, DEF, and NMP, as structure-directing agents, several extended MOFs, including some ZMOFs, have been successfully realized. Unlike the inorganic zeolite synthesis, the SDAs in the zinc(II) imidazolate synthesis are polar solvents rather than the organic amines, but like the inorganic zeolite synthesis, more than two different structures of zinc(II) imidazolate can be produced by using one SDA. Of them, only the thermodynamically controlled stable or quasi-stable MOFs can be produced in bulk. Fortunately, a dynamically controlled MOF directed by a SDA may be the thermodynamically controlled stable or quasi-stable MOF directed by another SDA. Thus, exploring for new SDAs has to be the key to creating new ZMOFs and bulk product of zinc(II) imidazolates. Also, introduction of substituents into the imidazolate ligands is another powerful strategy that may lead to generation of ZMOFs with high thermal stability. However, the substituents introduced may hinder the free rotation of Zn–N bonds, leading to a lack of framework diversities in the proposed zinc imidazolate derivates. Elimination of this conflict will be the next object of our studies, leading to the creation of ZMOFs with high thermal stability.

So far, the MOFs of metal(II) imidazolates and imidazolate derivates have been discovered with more than 20 different mineral topologies, of which several are the zeolitic topologies that account for most of the ZMOFs explored to date. This result has strongly supported our initial motivation in using metal (cobalt(II) and zinc(II)) imidazolate as the metal–organic analogues of inorganic silica. However, in contrast to more than 160 of zeolites and zeolite-related substances,[6] the ZMOFs obtained from metal imidazolate so far represent only a small number. Consequently, further extensive ZMOFs of metal(II) imidazolates and imidazole derivates can certainly be expected: they should be ZMOFs with the topologies of natural and synthetic zeolites or even the unprecedented zeolitic topologies. With respect to the ZMOFs constructed from other coordination polymers, the possibility also exists provided a metal (or a ligand) functions as the tetrahedral vertex, an *exo*-bidentate ligand (or metal) serves as the linker angled with about 145° and the coordination bonds possess the flexibility of rotation.

## Experimental Section

**General synthetic procedure**: All chemicals and solvents used in the syntheses were from commercial sources and used without further purification, but the solvents and organic amines were dried over 4–5 Å molecular sieves before use. The elemental analyses were carried out on a Perkin–Elmer 2400 elemental analyzer. The IR spectra were recorded (400–4000 $cm^{-1}$ region) on a FT-IR spectrometer TENSOR 27. XRD analyses were carried out on a Bruker D8 Advance and TGA (thermal gravimetric analyses) was performed under air with a heating rate of 5 °C $min^{-1}$ by using a Perkin–Elmer Diamond Thermogravimetric Analyzer. The syntheses of zinc imidazolates were carried out at room temperature: corresponding to the solvothermal synthesis of metal imidazolates, we name the room temperature synthesis as the nonsolvothermal synthesis which consists of 1) liquid diffusion for producing single crystals

  

used in X-ray single-crystal diffraction analysis and 2) liquid mixing for bulk microcrystals used for the XRD, elemental, and TG anaylses. The typical nonsolvothermal syntheses can be described as follows:

**Liquid diffusion**: Imidazole (0.068 g, 1.0 mmol) dissolved in the chosen SDA (3.0 mL) was placed in the bottom of a 5.0 mL test tube. Then, a solution of zinc(II) acetate dihydrate (0.11 g, 0.5 mmol) dissolved in propylamine (2.0 mL) was carefully layered over the SDA solution. Several days or even more than a week later, single crystals of zinc(II) imidazolates had grown to a size suitable for X-ray single-crystal determination.

**Liquid mixing**: In a 25 mL vessel, a solution of zinc(II) acetate dihydrate (0.22 g, 1.0 mmol) dissolved in propylamine (3.0 mL) was added dropwise into a solution of imidazole (0.136 g, 2.0 mmol) dissolved in the chosen SDA (6.0 mL). After about 40 min or even several days stirring at room temperature, the MOF of zinc(II) imidazolates formed were filtered and dried in a vacuum. The structural types of the microcrystalline MOFs of zinc imidazolates obtained were identified by comparing their XRD patterns with those simulated on the single-crystal data (see Supporting Information).

**Complex 1a**: Single crystals (pure phase) of **1a** were prepared under solvothermal conditions by using DEF as SDA and piperazine as BA. The bulk microcrystals (pure phase) of **1a** were prepared by the liquid-mixing method in DEF for 5 days, for which zinc(II) acetate dihydrate (0.88 g, 4.0 mmol) and imidazole (0.544 g, 8.0 mmol) were used, but the amount of DEF and propylamine was as same as that described in the general procedure (yield ca. 65% based on zinc). Elemental analysis calcd (%) for $C_{40}H_{52}N_{22}O_2Zn_5$ ($[Zn_5(im)_{10}\cdot 2DEF]_\infty$; 1199.89): C 40.04, H 4.37, N 25.69; found: C 40.11, H, 4.30, N 25.29; IR (KBr pellet): $\tilde{\nu}=3454$ (w, br), 3117 (w), 3106 (w), 2961–2874 (s), 1604 (w), 1496 (s), 1473 (s), 1383–1322 (w), 1281 (s), 1172 (w), 1088 (vs), 1029 (vs), 954 (s), 910 (m), 836 (m), 760 (s), 669 $cm^{-1}$ (s).

**Complex 2a**: The single crystals and the bulk microcrystals (pure phase) were prepared in DMA by liquid diffusion and liquid mixing, respectively (yield: ca.81% based on zinc). Elemental analysis calcd (%) for $C_{16}H_{21}N_9OZn_2$ (486.16): C 39.53, H 4.35, N 25.94; found: C 39.83, H 3.90, N 25.53; IR (KBr pellet): $\tilde{\nu}=3438$ (w, br), 3101 (w, sh), 2931 (w), 1646 (s), 1497 (s), 1410 (m, sh), 1395 (m, sh), 1319 (w, sh), 1285 (w, sh), 1240 (m, sh), 1172 (m, sh), 1087 (vs), 1014 (w, sh), 977 (w, sh), 953 (s), 839 (w, sh), 830 (w, sh), 766 (m), 753 (m), 672 (s) 588 $cm^{-1}$ (w).

**Complex 3a**: The single crystals and the bulk microcrystals (pure phase) were prepared in DMF by liquid diffusion and liquid mixing, respectively (yield: ca. 78% based on zinc). Elemental analysis calcd (%) for $C_{15}H_{19}N_9OZn_2$ (472.13): C 38.16, H 4.06, N 26.71; found: C 38.58, H 3.71, N 26.34; IR (KBr pellet): $\tilde{\nu}=3434$ (w), 3118 (w), 3100 (w), 2940 (w), 1681 (s), 1498 (s), 1480 (s), 1387 (w), 1321 (w), 1243 (w), 1171 (w), 1089 (vs), 955 (s), 836 (w), 757 (m), 670 $cm^{-1}$ (s).

**Complex 4a**: The single crystals were obtained by the liquid diffusion in DMF at a room temperature below 15 °C. No bulk microcrystals (pure phase) were obtained at this point.

**Complex 5a**: The single crystals can be prepared by liquid diffusion in DMA, DMF, and NMP. It should be noted that the liquid diffusion for gaining crystals suitable for X-ray diffraction must be conducted at a temperature below 15 °C if DMA or DMF are used as SDAs. However, if NMP is used as SDA, the single crystals (pure phase) suitable for X-ray diffraction can be obtained at ambient room temperature. The bulk microcrystals (pure phase) were prepared by liquid mixing in NMP for about one hour. Elemental analysis calcd (%) for $C_{11}H_{17}N_5O_2Zn$ ($[Zn(im)_2\cdot NMP\cdot(H_2O)]$; 316.69): C 44.24, H 5.06, N 23.45; found: C 44.25, H 5.29, N 22.64; IR (KBr pellet): $\tilde{\nu}=3453$ (w, br), 3103 (w, sh), 2925–2877 (m), 1681 (vs), 1496 (s), 1402 (m, sh), 1317–1249 (s, sh), 1170 (m, sh), 1087 (vs), 977 (m, sh), 953 (s), 832 (m), 830 (m), 759 (s), 670 (s) 560 (w), 471 $cm^{-1}$ (m, sh).

**Complex 6a** The single crystals and the bulk microcrystals (pure phase) were prepared by liquid diffusion and liquid mixing in DEF, respectively (yield: ca. 81% based on zinc). Elemental analysis calcd (%) for $C_{40}H_{52}N_{22}O_2Zn_5$ ($[Zn_5(im)_{10}\cdot 2DEF]_\infty$; 1199.89): C 40.04, H 4.37, N 25.69; found: C 40.55, H, 4.06, N 26.15; IR (KBr pellet): $\tilde{\nu}=3433$ (w, br), 3120 (w), 3110 (w), 2975 (w), 1667 (vs), 1591 (w), 1496 (s), 1489 (s), 1400 (w, sh), 1319 (w, sh), 1242 (m, sh), 1172 (m, sh), 1087 (vs), 1014 (w, sh), 977 (w, sh), 953 (s, sh), 831 (m), 759 (s), 670 $cm^{-1}$ (s).

**Complex 7a**: The single crystals were obtained by liquid diffusion in DEF at a room temperature below 15 °C. However, if tetramethylammonium bromide (ca. 2 mmol) was added in the reactant mixture, single crystals of **7a** were more likely to be obtained. The bulk product (pure phase) of this structure was not obtained at this point.

**Single-crystal X-ray structure determination**: Crystallographic measurements were carried out on a Bruker SMART CCD diffractometer with graphite-monochromated $Mo_{K\alpha}$ radiation ($\lambda=0.71073$ Å) at 293 K. The structures were solved by direct methods and refined by full-matrix least-squares techniques on $F^2$.[23] Non-hydrogen atoms of the MOFs of all metal(II) imidazolates were refined anisotropically except for disordered atoms. Hydrogen atoms on carbon atoms were generated geometrically and refined isotropically. Crystallographic data and information are presented in Table 2.

CCDC-254157–CCDC-254162 (**2a**–**7a**, respectively) contain the supplementary crystallographic data for this paper. These data can be obtained free of charge from The Cambridge Crystallographic Data Centre via www.ccdc.cam.ac.uk/data_request/cif.

## Acknowledgements

We are grateful to the Postdoctoral Foundation of China (No. 2003034003) and the National Science Foundation of China (No. 20571013) for the financial support.

[1] a) B. F. Hoskins, R. Robson, *J. Am. Chem. Soc.* **1990**, *112*, 1546; b) S. R. Batten, R. Robson, *Angew. Chem.* **1998**, *110*, 1558; *Angew. Chem. Int. Ed.* **1998**, *37*, 1460; c) S. S. Y. Chui, S. M. F. Lo, J. P. H. Charmant, A. G. Orpen, I. D. Williams, *Science* **1999**, *283*, 1148; d) H. Li, M. Eddaoudi, M. O'Keeffe, O. M. Yaghi, *Nature* **1999**, *402*, 276; e) B. Chen, M. Eddaoudi, S. T. Hyde, M. O'Keeffe, O. M. Yaghi, *Science* **2002**, *295*, 469; f) O. M. Yaghi, M. O'Keeffe, N. W. Ockwig, H. K. Chae, M. Eddaoudi, J. Kim, *Nature* **2003**, *423*, 705; g) S. Kitagawa, R. Kitaura, S.-I. Noro, *Angew. Chem.* **2004**, *116*, 2388; *Angew. Chem. Int. Ed.* **2004**, *43*, 2334.

[2] a) B. F. Abrahams, B. F. Hoskins, R. Robson, *Nature* **1994**, *369*, 727; b) D. Venkataraman, S. Lee, J. Zhang, J. S. Moore, *Nature* **1994**, *371*, 591.

[3] a) G. Férey, C. Serre, F. Millange, S. Surble, J. Dutour, I. Margiolaki, *Angew. Chem.* **2004**, *116*, 6456; *Angew. Chem. Int. Ed.*. **2004**, *43*, 6296; b) Q. Fang, G. Zhu, M. Xue, J. Sun, Y. Wei, S. Qiu, R. Xu, *Angew. Chem.* **2005**, *117*, 3913; *Angew. Chem. Int. Ed.* **2005**, *44*, 3845.

[4] a) X. C. Huang, J. P. Zhang, X. M. Chen, *Chin. Sci. Bull.* **2003**, *48*, 1491; b) J. A. R. Navarro, E. Barea, J. M. Salas, N. Masciocchi, S. Galli, A. Sironi, C. O. Ania, J. B. Parra, *Inorg. Chem.* **2006**, *45*, 2397.

[5] X. D. Guo, G. S. Zhu, Z. Y. Li, Y. Chen, X. T. Li, S. L. Qiu, *Inorg. Chem.* **2006**, *45*, 4065.

[6] The databases of zeolite structures can be found on the website: http://www.iza-structure.org/databases.

[7] R. Szostak, *Molecular Sieves: Principle of Synthesis and Identification*, van Nostrand Reinhold, New York, **1989**.

[8] Y. Q. Tian, Ph.D. Thesis, Nanjing University, **2002**.

[9] a) Y. Q. Tian, C. X. Cai, Y. Ji, X. Z. You, S. M. Peng, G. S. Lee, *Angew. Chem.* **2002**, *114*, 1442; *Angew. Chem. Int. Ed.* **2002**, *41*, 1384; b) Y. Q. Tian, C. X. Cai, X. M. Ren, C. Y. Duan, Y. Xu, S. Gao, X. Z. You, *Chem. Eur. J.* **2003**, *9*, 5673; c) Y.-Q. Tian, Z. X. Chen, L.-H. Weng, H. B. Guo, S. Gao, D. Y. Zhao, *Inorg. Chem.* **2004**, *43*, 4631.

[10] a) N. Masciocchi, S. Bruni, E. Cariati, F. Cariati, S. Galli, A. Sironi, *Inorg. Chem.* **2001**, *40*, 5897; b) N. Masciocchi, S. Galli, A. Sironi, *Comments Inorg. Chem.* **2005**, *26*, 1.

[11] X.-C. Huang, Y.-Y. Lin, J. P. Zhang, X.-M. Chen, *Angew. Chem.* **2006**, *118*, 1587; *Angew. Chem. Int. Ed.* **2006**, *45*, 1557.

  

[12] Y. Liu, V. C. Kravtsov, R. Larsen, M. Eddaoudi, *Chem. Commun.* **2006**, 1488.
[13] Y.-Q. Tian, L. Xu, C. X. Cai, J. C. Wei, Y. Z. Li, X. Z. You, *Eur. J. Inorg. Chem.* **2004**, 1039.
[14] B. B. McCusker in *Comprehensive Supramolecular Chemistry, Vol. 7* (Eds.: J. L. Atwood, J. E. D. Davis, D. D. MacNicol, F. Vögtle, F Toda, R. Bishop), Pergamon, Oxford, **1996**, pp. 393–423.
[15] M. O'Keeffe, H. Li, M. Eddaoudi, T. Reineke, O. M. Yaghi, *J. Solid State Chem.* **2000**, *152*, 3.
[16] J. Chen, R. H. Jones, S. Natarajan, M. B. Hursthouse, J. M. Thomas, *Angew. Chem.* **1994**, *106*, 667; *Angew. Chem. Int. Ed. Engl.* **1994**, *33*, 639.
[17] X. Bu, P. Feng, T. E. Gier, G. D. Stucky, *J. Solid State Chem.* **1998**, *136*, 210.
[18] X. Bu, P. Feng, T. E. Gier, D. Zhao, G. D. Stucky, *J. Am. Chem. Soc.* **1998**, *120*, 13389.
[19] J. V. Smith, *Chem. Rev.* **1988**, *88*, 149.
[20] C. Baerlocher, W. M. Meier, *Helv. Chim. Acta* **1970**, *53*, 1285.
[21] J. J. Pluth, J. V. Smith, J. M. Bennett, *J. Am. Chem. Soc.* **1989**, *111*, 1692.
[22] K. Fischer, V. Schramm, *Adv. Chem. Ser.* **1971**, *101*, 250.
[23] G. M. Sheldrick, SHELXTL-Plus V5.1 software Reference Manual, Bruker AXS Inc., Madison, WI, **1997**.

Received: February 2, 2007
Published online: March 30, 2007

  